Contamination, sources and risk assessments of metals in Stream Sediments of Pouma, Pan African Fold Belt, Southern Cameroon

Ndema Mbongué Jean-Lavenir (jndema2012@gmail.com)
University of Buea
Tume Noela Kiki
University of Buea
Lemnyuy Prosper Yiika
The University of Bamenda
Godlove Muh Ndi

Research Article

Keywords: Pouma, heavy metal, risk assessment, stream sediment, metal contamination

Posted Date: October 5th, 2022

DOI: https://doi.org/10.21203/rs.3.rs-2107911/v1

Abstract

The Pouma area is situated within the Yaoundé domain of the Pan Africa Fold Belt in Cameroon. The rocks in the Pouma area are mainly metamorphic rocks such as quartzite, micaschist and gneiss. The main objective of this study is to evaluate the distribution of trace metals and to assess the degree of metal pollution in the sediments of Pouma area. The sediment samples were analysed for major, trace elements and rare earth elements content byInductively Coupled Plasma-Mass Spectrometer (ICP-MS- Aqua Regia). The calculated pollution load index (1.1 to 8.1), enrichment factor (0.01 to 1221), integrated nemrow pollution load index (3.57 to 25.93) and potential ecological risk index (3 to 7504) of Au, Ag, Al, Ba, Bi, Cd, Co, Cu, Cr, Fe, Hg, Ga, Mo, Nb Ni, Pb, Rb, Sc, Sn, Sr, Th, U, V, Y, Zn and Zr indicate metal pollution and sediments contamination in the Pouma area. Natural and metal input assessment reveals that the dominantly mafic lithologies in the area, mining and domestic activities as well as agricultural activities of Pouma area are the main source of metal contamination.

Highlights

- The Pouma area is made up of metamorphic rocks that include quartzite, micaschist and gneiss
- The pollution parameters obtained in the Pouma area indicate metal pollution and sediment contamination
- Natural and anthropogenic metal input are the main source of metal contamination in Pouma area

1 Introduction

Environmental pollution is among the main challenges of today's society and is a major source of living organism's health problems (Wang and Zhou 2021). Heavy metal contamination of surface sediments is a major problem faces fast developing towns since sediment quality do not grow along with increase population, industrialization and urbanization. Among environmental contaminants, heavy metals gained special visibility due to the excessive concentrations, non/low-degradability, persistence, bio/ accumulative nature, and harmful effects on living organisms (Fuentes et al. 2020, Taati et al. 2020). Geological weathering, industrial disposal of metals and metal components, leaching of metals from garbage, solid waste heaps, mining, agriculture, pharmaceutical, domestic effluents, atmospheric sources, unplanned urbanization, haphazard industrialization, animal and human excreta are major sources of heavy metals and rare earth element (Chung 2018). The most important input of rare earth elements (REEs) in the aquatic environment include fertilizers used in agriculture, intensive use in the industry, specific medical applications and dry deposition of aerosol particles (Sojka et al. 2020; Liu et al. 2021). Trace elements and rare earth elements pollution in the river environment can also have adverse effects on organisms and humans, enter the food chain, and accumulate in aquatic organisms, sometimes at harmful levels (Adeel et al. 2019; Chan et al. 2021). The presence of trace elements or heavy metals in the aquatic ecosystems is widely reported and both abiotic and biotic processes affect their distribution and circulation (Moiseenko et al. 2019). Many studies have shown that nearly 90% of trace metal contaminants in a river system are usually associated with sediments (Argyraki et al. 2018), and between 10 and 60% of the sediments discharged into the river systems can be deposited and stored within the river channels and on the floodplains bordering the channels (Owens et al. 1997). Sediments are complementary and are equally vital parts of aquatic environments acting as carriers and potential sink for various pollutants. Many contaminants such as hazardous and toxic metals are accumulated in sediments, which could be extremely harmful to the aquatic environments (Pejman et al. 2015) As such, sediments serve as sensitive indicators for monitoring contaminants in aquatic environments. Heavy metals in stream sediments have negative effects on the river system due to their high toxic nature, reactivity and bioaccumulation. Sediments are major sink for heavy metals and other metalloids into the ecosystem. Comprehensive methods for identifying and assessing the severity of sediment contamination have been introduced in order to protect the aquatic life community (El-Taher et al. 2006). The main objective of this work is to evaluate the distribution of trace metals and rare earth elements and to assess the level of pollution in the sediments of Pouma area.

2 Geologic Setting

The Central African Orogenic Belt is a Neoproterozoic orogen linked to the Trans-Saharan belt of western Africa and to the Braziliano Orogen of northeastern Brazil (Van Schmus et al. 2008; Wang et al. 2019). In Cameroon, the Pan-African fold belt (Neoproterozoic fold belt) is made up of three geodynamic units (Fig. 1) namely (i) the northern domain consists of metasediments known as the Poli series which is associated with subordinate 830Ma-old volcanics of tholeiitic and alkaline affi nities. Widespread 630–660 Ma-old calc-alkaline granitoids were transformed to gneisses. (ii) the central domain is positioned between the Sanaga fault to the south and the Tcholliré-Banyo fault to the north. These large NE-striking transcurrent faults, as well as the Adamaoua fault inside the central domain, are regarded as possible prolongations of the major shear zones of NE Brazil in a pre-drift Gondwana reconstruction (Castaing et al. 1994), (iii) the

southern domain which contains the present study area, consists of an extensive tectonic nappe that was thrusted onto the Congo Craton (CC) during the Pan-African collision (Toteu et al. 2004; Fig. 1). It comprises low- to high-grade garnet-bearing schists, gneisses, and orthogenesis metamorphosed under a medium- to high pressure metamorphism reaching the granulite facies (Toteu et al. 2004). The low- to high- grade metasedimentary sequences of the Yaoundé Basin were intruded by syn- to late-tectonic mafic and felsic magmatic rocks between 620 and 590 Ma (Nkoumbou et al. 2014; Li et al. 2017; Fuh et al. 2021a). The southern domain includes the Yaoundé series (Nédelec et al. 1986) and extends in CAR with the Bolé series and the Gbaya high-grade gneisses and orthogneisses (Poidevin 1991). The Yaoundé group is made up of two series: Mbalmayo-Bengbis-Ayos and the Yaoundé series. Paragneisses and orthogneisses are predominant in the Yaoundé series. The schists and gneisses of the Yaoundé series were interpreted as Neoproterozoic epicontinental deposits related either to an intracontinental distensive environment or to a passive margin (Nzenti et al. 1988). Sm–Nd isotopic data (Toteu et al. 2001) indicate that the presumed metasediments and meta-igneous rocks were derived from a protolith consisting of a mixture of juvenile Neoproterozoic and Paleoproterozoic sources without major contribution from the Congo Craton. The only possible source for old components is represented by the Paleoproterozoic basement of north-central Cameroon, suggesting that the Yaoundé series formed in the internal zone of the Pan-African fold belt before being thrust onto the Congo Craton (Toteu et al. 2004). Geochemical studies based on isotopic data suggest that the Yaoundé Group is Late Neoproterozoic in age (626 Ma) and comprises a mixture of detritus from a Paleoproterozoic crust and from Neoproterozoic sources (Toteu et al. 2006). U-Pb dating of metamorphic rutile, monazite, and zircon revealed different episodes of metamorphism and deformation of sediments between 650 and 560 Ma (Owona et al. 2011; Betsi et al. 2020) that reached a metamorphic peak at 620 Ma (Toteu et al. 2004). The model ages from Sm-Nd and Lu-Hf isotopes indicate a Paleoproterozoic crustal source for the Letta granite and Yaoundé orthogneiss with Nd_{TDM} and Hf_{TDM} ranging from 1.8 to 1.9 Ga and 1.7 to 2.0 Ga, respectively (Toteu et al. 2004; Li et al. 2017).

3 Methods

Sediment concentrates were obtained by panning active stream sediment samples collected at various points along catchment areas and tributaries of the studied area. A total of 12 stream sediment samples were taken at a depth of 30–70 cm down the stream beds to avoid contamination. The panned sediment concentrates were immediately transferred into polyethylene bags and transported to the laboratory. Once in the laboratory, these samples were air-dried at 40˚C, homogenized in an agate mortar and passed through a 2 mm plastic sieve to remove plant parts, debris and gravel-sized materials. 0.5g of the powder sample is digested in aqua regia in a microprocessor-controlled digestion block. The sample is then cooled and diluted to 10 ml with deionized water and homogenized. The digested samples were then analysed for major, trace elements and rare earth elements content by Inductively Coupled Plasma-Mass Spectrometer (ICP-MS- Aqua Regia) after digestion of the samples. One blank is run for every 12 samples. An in-house control is run every 12 samples. Digestion and ICP-MS analysis of samples were done at Activation Laboratories (ACTLABS) Ltd., Ontario in Canada.

4 Results And Discussion

4.1 Major elements

Results of the major element analyses are presented in Table 1. Fe_2O_3 (0.45 to 8.86 wt% with a mean of 2.94) show moderate enrichment when compared with the recommended values of the Upper Continental Crust (UCC) by Rudnick and Gao (2003). P_2O_5 (0–0.4w % with mean of 0.01) and SO_3 (0.20 wt %) display uniform and constant low concentrations. The alkali and alkaline earth oxides values (Na_2O + CaO + K_2O + MgO) are less than those proposed by Rudnick and Gao (2003). Moderate enrichment of Fe_2O_3 when compared with Rudnick and Gao (2003) in sediments indicate that the sediments are highly ferruginous and should come from ferromagnesian minerals such as biotite, garnet, sillimanite and iron oxide. The low contents of alkali and alkali-earth oxides (MgO, K_2O, CaO, and Na_2O) result from their high mobility during weathering (Torres-Alvarado et al. 2007). The chemical composition of the studied stream sediment samples is reported in the enrichment-depletion plot (Fig. 2) in which samples show slightly enrichment in SO_3 and Fe_2O_3 and depletion for the rest of major elements.

Table 1
Major oxides composition in stream sediments of Pouma area

Sample	PM02	PM03	PM04	PM05	PM06	PM07	PM08	PM09	PM010	PM011	PM012	PM013
Al_2O_3 (%)	0.59	0.25	0.57	0.27	0.42	0.3	0.37	0.37	0.25	0.05	0.22	0.27
Fe_2O_3	3.16	2.53	4.46	2.04	2.47	3.41	8.86	2.2	1.73	0.45	2.03	1.93
MgO	0.04	0.01	0.05	0.03	0.07	0.07	0.1	0.07	0.04	0.01	0.02	0.04
CaO	0.94	0.36	0.45	0.31	0.46	0.16	0.24	0.3	0.26	0.02	0.27	0.27
Na_2O	0.05	0.03	0.28	0.02	0.03	0.03	0.02	0.03	0.02	0.02	0.02	0.02
K_2O	0.02	0.02	0.12	0.02	0.02	0.02	0.02	0.02	0.02	0.02	0.02	0.01
TiO_2	0.49	0.42	0.38	0.36	0.36	0.19	0.26	0.21	0.23	0.08	0.37	0.26
P_2O_5	0	0	0	0	0.01	0.04	0.01	0.03	0.01	0.03	0.01	0.02
SO_3	0.2	0.2	0.2	0.2	0.2	0.2	0.2	0.2	0.2	0.2	0.2	0.2
Au (ppb)	10	0.68	0.13	0.8	0.87	0.17	0.04	0.15	0.03	0.09	0.02	0.05
Ag (ppm)	1.49	0.14	0.06	0.28	0.3	0.05	0.04	0.05	0.02	0.03	0.02	0.03
Ba	8.5	9.1	16.2	7.9	10.3	5.9	10.9	7	5.8	5.3	8.3	9.9
Bi	0.07	0.05	0.08	0.07	0.09	0.06	0.08	0.3	0.07	0.06	0.1	0.07
Cd	0.08	0.03	0.05	0.08	0.15	0.04	0.14	0.09	0.08	0.01	0.04	0.1
Co	11.5	3	4.9	2.1	2.4	6	22.6	2.5	1.8	1.6	2.3	2.3
Cr	26	16	35	12	17	44	80	17	12	5	13	14
Cu	17.5	6	22.5	4.2	3.4	5.5	57.5	150	2.9	3.5	4	3.1
Ga	7.01	2.97	4.7	1.78	2.27	0.13	4.66	0.29	1	0.02	1.35	0.72
Hg (ppb)	1.83	0.29	0.25	0.66	0.61	0.71	1.3	1.69	0.38	0.34	0.76	0.56
Mn	720	596	635	616	882	810	887	824	586	142	642	683
Mo	0.17	0.06	0.13	0.18	0.21	0.36	0.67	0.37	0.25	0.12	0.16	0.17
Li	0.8	0.1	3.1	8.1	0.4	0.3	0.3	0.4	0.1	0.1	0.1	0.1
Ni	4	1.9	4.3	1.2	1.6	3.5	17.6	1.8	1.3	1	1.3	1.6
Pb	18.4	53.9	7.7	10.2	7.1	16.1	18.4	16.3	8.4	14.6	8.6	10.3

Table 1
Continued

Rb	**0.9**	**0.7**	**3.3**	**0.4**	**0.5**	**0.6**	**0.7**	**0.5**	**0.4**	**0.5**	**0.5**	**0.5**
Sc	9.6	4.6	5.3	4.6	8.7	5.3	7.1	6.7	4.7	1.1	4.6	5
Sn	1.22	1.01	5.09	0.5	0.45	1.79	2.67	4.49	0.53	0.71	0.7	0.48
Sr	106	45.2	45.2	29.5	40.2	6.6	12.4	19.9	24.6	3	26.7	23.8
Th	12.6	21.9	19.9	32.8	76.2	200	52.9	200	128	200	106	162
Te	0.02	0.02	0.02	0.02	0.02	0.02	0.02	0.02	0.02	0.02	0.02	0.02
U	1.5	1.5	1.5	3.9	9	31.5	4.2	26.2	14.7	21.4	11.7	19.2
V	47	22	43	14	20	52	85	17	15	5	17	16
Y	16.2	9.62	10.3	11.2	18.3	21.4	14.9	23.8	14.9	101	15.3	18
Zn	22.1	24.3	23.8	18.5	19.3	16.3	25.3	15	14.4	3.8	18	15.4
Zr	174	171	40	33.2	26.6	2	33.6	1.8	5.1	0.8	11.9	4.3
La	41.4	43.2	39.6	103	204	744	107	609	358	714	277	456
Ce	84.4	91.6	85	199	449	1640	234	1320	786	1590	614	1000
Pr	8.9	9.3	8.7	20.8	50.1	174	23.6	140	83.1	168	69.8	109
Nd	33	34.8	32.9	86.9	190	647	91.3	529	327	643	250	415
Sm	5.9	5.5	4.9	13.6	29	93.6	16.2	80.8	41.7	100	40.1	57.2
Eu	1.1	0.6	0.7	1.6	3.4	11.7	1.6	9.5	5.8	10.6	4.7	7.4
Gd	4.9	4.3	4	9.6	19.4	63.1	9.7	53.2	30.6	80.1	25.9	40.5
Tb	0.6	0.4	0.4	0.8	1.4	3.8	0.8	3.2	1.9	7.7	1.7	2.6
Dy	3.5	2.1	2.2	2.6	4.7	8.3	3.3	7.7	4.9	32.8	4.8	6.3
Ho	0.6	0.4	0.4	0.4	0.7	0.7	0.5	0.8	0.5	4.2	0.6	0.6
Er	1.7	0.9	1.2	1.2	1.9	1.6	1.6	2	1.3	8.1	1.2	1.4
Tm	0.2	0.1	0.1	0.2	0.2	0.2	0.2	0.3	0.2	0.8	0.2	0.2
Yb	1.6	0.9	1.1	1.1	1.8	1	1.5	1.6	1	3.8	1.1	1.2
Lu	0.2	0.1	0.2	0.2	0.2	0.2	0.2	0.2	0.1	0.5	0.2	0.2
∑REE	188	194.2	181.4	441	955.8	3389.2	491.5	2757	1642.1	3363.6	1291.3	2097.6
$(La/Sm)_N$	1.05	1.18	1.21	1.14	1.06	1.19	0.99	1.13	1.29	1.07	1.04	1.2
$(La/Yb)_N$	1.9	3.52	2.64	6.87	8.31	54.56	5.23	27.91	26.25	13.78	18.47	27.87
$(Gd/Yb)_N$	1.77	2.77	2.11	5.05	6.24	36.53	3.74	19.25	17.72	12.2	13.63	19.54
Eu/Eu*	0.96	0.58	0.74	0.66	0.67	0.72	0.6	0.68	0.76	0.56	0.69	0.72

The Pearson's correlation matrix (Fig. 3) mostly show positive correlations for major elements. This indicate they result from similar sources. In addition, the correlation between TiO_2 and CaO and Al_2O_3, Na_2O and Al_2O_3, Al_2O_3 and K_2O and CaO could be link to the present of minerals like feldspars, rutile, ilmenite, kyanite and andalusite in metamorphic rocks of the study area. The correlation of Fe_2O_3 and MgO could probably be due to the presence of mafic minerals such as garnet boitite, garnet and sillimanite in relation to metamorphic rocks of the study area

4.2 Trace elements

The concentration of trace elements in stream sediment of Pouma is reported in Table 1. The stream sediments show high content in Mn (142–887 ppm, average = 668.58 ppm, Th (12–200 ppm av. = 101 ppm), Zr (0.8–174 ppm av. = 42 ppm), Sr (3–106 ppm, av. = 31.93 ppm), V (5–85 ppm av. = 29.42 ppm), Y (9.62–101 ppm av. = 22.91 ppm) respectively, greatly exceed the standard proposed by Rudnick and Gao (2003). The high mean concentration of these elements could be attributed to intense weathering of the parent rocks, phosphate fertilizers, pesticides, fungicides, sewage sludge, garbage and waste water irrigation in Pouma area. The content of the other trace elements is lower than reference values (Rudnick and Gao 2003). Comparism between the mean values of metals traces in the various samples shows that Mn, Sr, Th and Zr concentrations are higher than those of other metals. This reveals that a high concentration of Mn, Sr, Th and Zr in the sediments cannot be conclusively attributed to lithogenic influence alone, but have other sources. The concentration of the other trace elements is lower than the reference values (Rudnick and Gao, 2003). The contents of rare or poor metals such as Ga (0.02–7 ppm), Bi (0.05–0.3 ppm), Sn (0.48–4.49 ppm), are very low except Pb (7.1–53.9 ppm) which is slightly elevated. The low mean concentration of other metals and radioactive elements can be linked to leaching from source rocks during weathering and high mean concentration of Mn, Sr, Th, V and Zr could be attributed to intense weathering of the parent rocks, phosphate fertilizers, pesticides, fungicides, sewage sludge, garbage and waste water irrigation in Pouma area (Singh et al. 2017, Ekoa Bessa et al. 2018). The content of some transition metals could be linked to the occurrence of quartzite, mica-schist and gneiss in the study area (Etame et al. 2013), while the enrichment of Hg, Pb, Th and U is probably due to anthropogenic activities such as mining, agricultural activities, municipal and household waste, sewage sludge and urbanization (Singh et al. 2017; Ekoa Bessa et al. 2018).

The majority of trace elements show positive correlations (Fig. 3). This positive correlation between elements ($r > 0.5$) could be attributed to parent rock (geologic unit), mining activities (mine tailings dump, oil and fuel used for heavy machine engines, the vestiges of abandoned machines, rusty empty barrels and plastic tins) and agricultural activities (used of phosphate fertilizers, pesticides, fungicide and animal manure) which are probably governed by the same or similar physicochemical processes (Emmanuel et al. 2014; Otari and Dabiri 2015) in the study area. The correlation coefficients of selected elements have been plotted and the similarity in the patterns for Ag and Zr; Ba, Y, Zn and V (Fig. 4) implies some geochemical coherence suggesting evidence for similar input sources and common geochemical characteristics of these trace elements.

4.3 Rare Earth Element (REE)

The chemical composition of rare earth element is shown in Table 1. The normalization to the upper continental crust (UCC) by McLennan (2001) was performed for the evaluation of the REE distribution in the investigated sediment samples and for a better comparison. The total REE contents (ΣREE) vary between 181 and 3364 ppm, it higher than those reported by (Loell et al. 2011) in soils of Japan, Australia and Germany. The REE follow the trend: Ce > La > Nb > Pr > Sm > Gd > Dy > Eu > Er > Yb > Tb > Ho > Tm > Lu in sediment samples of the study area (Table 1). The light rare earth element (La, Ce, Pr, Nd, Sm) in the sediments samples of the study area were significantly enriched relative to the UCC values while the other rare earth elements were depleted in the samples. The UCC normalized REE patterns (Fig. 5) show REE fractionation (La_N/Yb_N = 1.05–1.29), light rare earth element (LREE) enrichment (La_N/Sm_N = 2.64–54.56) relative to heavy rare earth element (HREE; Gd_N/Yb_N = 1.77–36.53 with a negative Eu anomaly (Eu/Eu* = 0.54–0.96). The high REE contents could be due to their absorption at the smectite and kaolinite interfaces (Ndjigui et al. 2014). This could also be attributed to complexation of REE with water carbon ligands (Khadijeh et al. 2009). The high La_N/Yb_N is due to the high fractionation of REE during weathering and erosion (Ramos-Vázquez et al. 2018). The enrichment of LREE in sediment samples could be associated with phosphate minerals (Hannigan et al. 2001) such as monazite, probably due to geological processes (Sholkovitz et al. 1995; Lecuyer et al. 2004; Zhang et al. 2012). It may also come from anthropogenic sources such as quarrying, the use of phosphate fertilizers in agricultural sites, suggesting possible source of contamination of REEs (Wang et al. 2019). The low HREE contents (Gd, Dy, Eu, Er, Yb, Tb and Lu) may be due to non-hosted REE minerals (xenotime, quartz) and rocks such as and quartzite (Nesbitt et al. 1996). The negative Eu anomalies could be due to the substitution of europium by strontium in clay minerals or in some heavy minerals such as zircon, rutile, garnet, kyanite, sillimanite and epidote (Etame et al. 2013).

4.4 Factor analysis

According to the Kaiser criterion, the factors with eigenvalues > 1 were taken into consideration for evaluations. Five factors that account for 88.74% of the total data cumulative variance has been recorded in the study area (Table 2). The elements in factor groups with the factor loading scores > 0.50 were interpreted to identify their possible sources. Factor 1 (Ag, Au, Ga, Hg, Sr, Zr), accounts for 34.954% of the total data variance. This factor is mainly loaded with chalcophile elements such as Ag, Hg and Au, two lithophile elements (Sr, Zr). It is related to the sulphidation and silicate events. Factor 2 (Co, Cr, Mo, Ni, V) is made up of siderophile elements accounting for 20.90% of the total variance. These elements grouping reflect their transition metal relationship and their availability in the environment. The presence of

Cr in factor 2 can be link by the presence of chromite in parent rocks. Factor 3 (Ba, Cs, Rb, Sn, Zn) acounts for 14.05 of the total data variance. It is mainly consist of two litophile elements elements (Ba, Cs, Rb) suggesting a silicate phase mineral or may be the high mobility of these elements within the environment. This factor represents the lithological controlled, the strong loading of Ba (0.89) may be due to the presence of feldspar in the study area. Cs (0.96) and Rb (0.870) could proven from assorted wastes produced from nuclear or radioactive materials. Factor 4 (Cd, Mn, Nb, Sc) accounts for 10.47% of the total data variance and also reflects a lithological controlled. Factor 5 (Bi, Cu, Sn) accounts for 8.26% of the total data variance, it has affinity with sulphide minerals.

Table 2
Factor analysis

Elements	F1	F2	F3	F4	F5
Ag	**0.94**	-0.01	-0.07	0.14	0.01
Au	**0.95**	0.02	-0.09	0.07	0.04
Ba	0.02	0.19	**0.89**	0.20	-0.06
Bi	-0.12	-0.14	-0.06	0.18	**0.93**
Cd	0.01	0.28	-0.02	**0.88**	0.07
Co	0.26	**0.94**	0.03	0.16	0.02
Cr	-0.04	**0.95**	0.19	0.16	0.07
Cs	0.16	-0.14	**0.96**	-0.05	0.06
Cu	-0.05	0.20	-0.01	0.10	**0.92**
Ga	**0.73**	0.41	0.48	0.14	-0.10
Hg	**0.53**	0.33	-0.29	0.31	**0.63**
Mn	0.08	0.34	0.17	**0.77**	0.30
Mo	-0.24	**0.81**	-0.22	0.34	0.31
Nb	0.18	0.35	-0.23	**0.84**	-0.09
Ni	0.00	**0.97**	0.10	0.16	0.01
Pb	0.36	0.16	0.06	-0.42	-0.08
Rb	-0.01	0.07	**0.87**	-0.27	0.09
Sc	**0.55**	0.22	0.14	**0.70**	0.26
Sn	-0.12	0.30	**0.59**	-0.13	**0.72**
Sr	**0.91**	-0.15	0.29	0.17	-0.03
Th	-0.56	-0.16	-0.60	-0.20	0.38
U	-0.51	-0.14	-0.57	-0.16	0.42
V	0.17	**0.91**	0.22	0.14	0.05
Y	-0.18	-0.08	-0.48	-0.62	0.01
Zn	0.38	0.41	**0.63**	0.38	-0.09
Zr	**0.88**	0.07	0.23	-0.16	-0.17
Eigen Value	9.086	5.459	3.655	2.723	2.149
% of Variance	34.948	20.995	14.059	10.472	8.266
Cumulative %	34.948	55.943	70.002	80.474	88.740

4.4 Heavy Metals Assessment in Stream Sediments

Pollution indices are very useful in processing, analysing, and conveying raw environmental information to the public and decision-makers (Caeiro et al. 2005). Numerous parameters were used to evaluate sediment pollution in the study area.

4.4.1 Contamination factor (CF) and Degree of contamination (Cdeg)

The (CF) was used to assess the pollution load of the sediments with respect to heavy metals. The CF for each metal was determined using the formula of by Hakanson (1980).

$$CF = \frac{\text{Concentrationofmetalinsample}}{\text{Backgroundconcentrationofmetal}}$$

The background value is a reference value for the maximum allowable concentration of metals in the crust (Rudnick and Gao 2003). The CF was interpreted as follows: low contamination at CF < 1; moderate contamination at 1 < CF < 3, considerable contamination at 3 < CF < 6, and very high contamination at CF > 6 (Kerolli *et al*., 2015). In order to evaluate sediment quality, the calculated CF shows that Au, Ag, Al, Ba, Bi, Cd, Co, Cu, Cr, Fe, Ga, Mo, Ni, PB, Rb, Sc, Sn, Sr, Th, U, V, Y, Zn and Zr are low in the study area (CF < 1) indicating low contamination for the sediments enriched in these elements. The CF values of Cd in sample (PM08), Pb (samples PM02, PM03 PM08), U (samples PM05 and PM08) and Y (sample PM09) shows moderate contamination (1 < CF < 3), while Th (in sample PM05), U (samples PM06, PM010 and PM12) and Y (sample PM11) are considerably contaminated (3 < CF < 6). Very high contamination (CF > 6) refers to Hg, Th and U (samples PM07, PM09, PM11 and PM13) in the study area (Table 3). Contamination in the study area could be attributed to lithogenic influence and anthropogenic activities such as quarrying.

Table 3
Calculated contamination factor (CF), Degree of contamination (Cdeg), Pollution load index (PLI) and integrated pollution load index (NIPI)

	PM02	PM03	PM04	PM05	PM06	PM07	PM08	PM09	PM010	PM011	PM012	PM013	Cdeg
Au	6.67	0.45	0.09	0.53	0.58	0.11	0.03	0.10	0.02	0.06	0.01	0.04	8.69
Ag	0.03	0.00	0.00	0.01	0.01	0.00	0.00	0.00	0.00	0.00	0.00	0.00	0.05
Al	0.07	0.03	0.07	0.03	0.05	0.04	0.05	0.05	0.03	0.01	0.03	0.03	0.48
Ba	0.01	0.01	0.03	0.01	0.02	0.01	0.02	0.01	0.01	0.01	0.01	0.02	0.17
Bi	0.44	0.31	0.50	0.44	0.56	0.38	0.50	1.88	0.44	0.38	0.63	0.44	6.88
Cd	0.89	0.33	0.56	0.89	1.67	0.44	1.56	1.00	0.89	0.11	0.44	1.11	9.89
Co	0.66	0.17	0.28	0.12	0.14	0.35	1.31	0.14	0.10	0.09	0.13	0.13	3.64
Cr	0.28	0.17	0.38	0.13	0.18	0.48	0.87	0.18	0.13	0.05	0.14	0.15	3.16
Cu	0.63	0.21	0.80	0.15	0.12	0.20	2.05	5.36	0.10	0.13	0.14	0.11	10.00
Fe	0.70	0.56	0.98	0.45	0.55	0.75	1.95	0.48	0.38	0.10	0.45	0.42	7.78
Ga	0.40	0.17	0.27	0.10	0.13	0.01	0.27	0.02	0.06	0.00	0.08	0.04	1.54
Hg	36.60	5.80	5.00	13.20	12.20	14.20	26.00	33.80	7.60	6.80	15.20	11.20	188
Mo	0.15	0.05	0.12	0.16	0.19	0.33	0.61	0.34	0.23	0.11	0.15	0.15	2.59

Table 3
Continued

Ni	**0.09**	**0.04**	**0.09**	**0.03**	**0.03**	**0.07**	**0.37**	**0.04**	**0.03**	**0.02**	**0.03**	**0.03**	**0.87**
Pb	1.08	3.17	0.45	0.60	0.42	0.95	1.08	0.96	0.49	0.86	0.51	0.61	11.18
Rb	0.01	0.01	0.04	0.00	0.01	0.01	0.01	0.01	0.00	0.01	0.01	0.01	0.11
Sc	0.69	0.33	0.38	0.33	0.62	0.38	0.51	0.48	0.34	0.08	0.33	0.36	4.81
Sn	0.58	0.48	2.42	0.24	0.21	0.85	1.27	2.14	0.25	0.34	0.33	0.23	9.35
Sr	0.33	0.14	0.14	0.09	0.13	0.02	0.04	0.06	0.08	0.01	0.08	0.07	1.20
Th	1.20	2.09	1.90	3.12	7.26	19.05	5.04	19.05	12.19	19.05	10.10	15.43	115
U	0.56	0.56	0.56	1.44	3.33	11.67	1.56	9.70	5.44	7.93	4.33	7.11	54
V	0.48	0.23	0.44	0.14	0.21	0.54	0.88	0.18	0.15	0.05	0.18	0.16	3.64
Y	0.77	0.46	0.49	0.53	0.87	1.02	0.71	1.13	0.71	4.81	0.73	0.86	13.09
Zn	0.33	0.36	0.36	0.28	0.29	0.24	0.38	0.22	0.21	0.06	0.27	0.23	3.23
Zr	0.90	0.89	0.21	0.17	0.14	0.01	0.17	0.01	0.03	0.00	0.06	0.02	2.61
PLI	3.2	2.4	5.5	2.3	8.1	1.1	1.6	2.7	1.7	2.4	1.3	4.8	
NIPI	25.93	4.13	3.57	9.36	8.67	13.55	18.43	24.00	8.66	13.52	10.79	10.97	

Table 4
Geo-accumulation index (Igeo) of heavy metals in sediment sediments of Pouma area

	PM02	**PM03**	**PM04**	**PM05**	**PM06**	**PM07**	**PM08**	**PM09**	**PM010**	**PM011**	**PM012**	**PM013**
Au	1.34	0.09	0.02	0.11	0.12	0.02	0.01	0.02	0.00	0.01	0.00	0.01
Ag	0.01	0.00	0.00	0.00	0.00	0.00	0.00	0.00	0.00	0.00	0.00	0.00
Al	0.01	0.01	0.01	0.01	0.01	0.01	0.01	0.01	0.01	0.00	0.01	0.01
Ba	0.00	0.00	0.01	0.00	0.00	0.00	0.00	0.00	0.00	0.00	0.00	0.00
Bi	0.09	0.06	0.10	0.09	0.11	0.08	0.10	0.38	0.09	0.08	0.13	0.09
Cd	0.18	0.07	0.11	0.18	0.33	0.09	0.31	0.20	0.18	0.02	0.09	0.22
Co	0.13	0.03	0.06	0.02	0.03	0.07	0.26	0.03	0.02	0.02	0.03	0.03
Cr	0.06	0.03	0.08	0.03	0.04	0.10	0.17	0.04	0.03	0.01	0.03	0.03
Cu	0.13	0.04	0.16	0.03	0.02	0.04	0.41	1.08	0.02	0.03	0.03	0.02
Fe	0.14	0.11	0.20	0.09	0.11	0.15	0.39	0.10	0.08	0.02	0.09	0.09
Ga	0.08	0.03	0.05	0.02	0.03	0.00	0.05	0.00	0.01	0.00	0.02	0.01
Hg	7.34	1.16	1.00	2.65	2.45	2.85	5.22	6.78	1.53	1.36	3.05	2.25
Mo	0.03	0.01	0.02	0.03	0.04	0.07	0.12	0.07	0.05	0.02	0.03	0.03
Ni	0.02	0.01	0.02	0.01	0.01	0.01	0.08	0.01	0.01	0.00	0.01	0.01

The degree of contamination (Cdeg) is defined as the sum of all contamination factors for various heavy metals. (Cdeg) was proposed by Hakanson (1980) which is obtained as follows:

$$Cdeg = \sum_{i=1}^{8} CF$$

Hakanson (1980) proposed this classification as follows: Cdeg < 6 indicates a low degree of contamination; 6 < Cdeg < 12 is a moderate degree of contamination; 12 < Cdeg < 24 is a considerable degree of contamination and Cd > 24 is a high degree of contamination. The results of degree of contamination is presented in Table 3. Cdeg in the study area follow the order: Hg > Th > U > Y > Pb > Cu > Cd > Sn > Au >

Fe > Bi > Sc > Co > V > Zn > Cr > Zr > Mo > Ga > Sr > Ni > Al > Ba > Rb > Ag. Ag, Al, Ba, Co,Cr, Ga, Mo,Ni, Rb,Sc, Sr, V, Zn, and Zr indicates low degree of contamination (Cdeg < 6) in sediments. Au, Bi, Cd, Cu, Fe, Pb and Sn shows moderate degree of contamination (6 < Cdeg < 12), while Y display considerable degree of contamination (12 < Cdeg < 24) in Pouma area. Hg, Th and U shows high degree of contamination (Cdeg > 24) in sediments of Pouma area indicating anthropogenic and geogenic sources of contamination.

4.4.2 Pollution load index (PLI) and integrated nemerow pollution load index (NIPI)

The PLI is used to find out the mutual pollution effect at various stations by the different elements in sediments. The PLI enable to make an assessment of the overall toxicity status of each sampling site in the study area. It is given according to Tomlinson (1980) by the relation

$PLI = (CF_1 \times CF_2 \times ..... \times CF_n)^{1/n}$

The PLI value of > 1 is polluted, whereas < 1 indicates no pollution and PLI values = 1 is perfection (Tomlinson 1980). The PLI across the study area was in the order: sample PM06 > PM04 > PM13 > PM02 > PM09 > PM03 > PM11 > PM05 > PM10 > PM08 > PM12 > PM07 with values 8.1, 5.5, 4.8, 3.2, 2.7, 2.4, 2.4, 2.3, 1.7, 1.6, 1.33 and 1.1 respectively. The PLI values varies from 1.1 in sample PM07 to 8.1 in sample PM06 indicating that sediments of the study area are highly polluted in these metals (Table 7, Fig. 3). The high level of PLI values observed might be due to the effects of human activities. It is presumed that the occurrence of metals in sediments is due to agricultural practices, use of phosphate fertilizers, discharge of effluents, mining activities, urbanization, untreated sewage and municipal waste into streams and rivers of the studied area.

Table 7
Anthropogenic input of heavy metals in sediments of Pouma area

	PM02	PM03	PM04	PM05	PM06	PM07	PM08	PM09	PM010	PM011	PM012	PM013
Au	666.67	45.33	8.80	53.40	58.07	11.13	2.72	9.80	2.08	6.08	1.26	3.57
Ag	2.81	0.26	0.10	0.53	0.56	0.08	0.08	0.08	0.03	0.06	0.03	0.05
Al	7.21	3.05	6.95	3.31	5.13	3.64	4.55	4.55	3.12	0.65	2.73	3.31
Ba	1.36	1.46	2.60	1.27	1.65	0.95	1.75	1.12	0.93	0.85	1.33	1.59
Bi	43.75	31.25	50.00	43.75	56.25	37.50	50.00	187.50	43.75	37.50	62.50	43.75
Cd	88.89	33.33	55.56	88.89	166.67	44.44	155.56	100.00	88.89	11.11	44.44	111.11
Co	66.47	17.34	28.32	12.14	13.87	34.68	130.64	14.45	10.40	9.25	13.29	13.29
Cr	28.26	17.39	38.04	13.04	18.48	47.83	86.96	18.48	13.04	5.43	14.13	15.22
Cu	62.50	21.43	80.36	15.00	12.14	19.64	205.36	535.71	10.36	12.50	14.29	11.07
Fe	69.64	55.75	98.41	45.04	54.56	75.20	195.44	48.41	38.10	9.92	44.84	42.46
Ga	40.06	16.97	26.86	10.17	12.97	0.74	26.63	1.66	5.71	0.11	7.71	4.11
Hg	3660	580	500	1320	1220	1420	2600	3380	760	680	1520	1120
Mo	15.45	5.45	11.82	16.36	19.09	32.73	60.91	33.64	22.73	10.91	14.55	15.45
Ni	8.51	4.04	9.15	2.55	3.40	7.45	37.45	3.83	2.77	2.13	2.77	3.40

Table 7
Continued

Pb	108.24	317.06	45.29	60.00	41.76	94.71	108.24	95.88	49.41	85.88	50.59	60.59
Rb	1.07	0.83	3.93	0.48	0.60	0.71	0.83	0.60	0.48	0.60	0.60	0.60
Sc	68.57	32.86	37.86	32.86	62.14	37.86	50.71	47.86	33.57	7.86	32.86	35.71
Sn	58.10	48.10	242.38	23.81	21.43	85.24	127.14	213.81	25.24	33.81	33.33	22.86
Sr	33.13	14.13	14.13	9.22	12.56	2.06	3.88	6.22	7.69	0.94	8.34	7.44
Th	120.00	208.57	189.52	312.38	725.71	1904.76	503.81	1904.76	1219.05	1904.76	1009.52	1542.86
U	55.56	55.56	55.56	144.44	333.33	1166.67	155.56	970.37	544.44	792.59	433.33	711.11
V	48.45	22.68	44.33	14.43	20.62	53.61	87.63	17.53	15.46	5.15	17.53	16.49
Y	77.14	45.81	49.05	53.33	87.14	101.90	70.95	113.33	70.95	480.95	72.86	85.71
Zn	32.99	36.27	35.52	27.61	28.81	24.33	37.76	22.39	21.49	5.67	26.87	22.99
Zr	90.16	88.60	20.73	17.20	13.78	1.04	17.41	0.93	2.64	0.41	6.17	2.23

The NIPI measures the level of pollution by metals and can estimate the effects of various metals in soil quality and the environment. The index is calculated using the following formula (Gao et al. 2016):

$$\mathrm{NIPI}_{Nemerow} = \frac{\sqrt{\left(\frac{1}{\mathrm{m}}\sum_{\mathrm{i}=1}^{\mathrm{m}}\mathrm{P_i}\right)^2 + \left(\mathrm{P_{imax}}\right)^2}}{2}$$

Where, P_i is the single pollution index of heavy metal i; P_{imax} is the maximum value of the single pollution indices of the investigated heavy metal(s) and m is the count of the heavy metal species. The quality of sediments were classified into five categories as follows: $NIPI_{Nemerow} < 0.7$, unpolluted (Clean), $0.7 \leq NIPI_{Nemerow} < 1.0$, little pollution (warning limit); $1.0 \leq NIPI_{Nemerow} < 2.0$, slight pollution (light pollution); $2.0 \leq NIPI_{Nemerow} < 3.0$, moderate pollution (medium pollution); $NIPI_{Nemerow} \geq 3.0$, serious pollution (heavy/high pollution; Gao et al., 2016). The NIPI across the study area varies from 3.57 in sample PM04 to 25.93 in sample PM02 (Table 3). The NIPI follow the trend: PM02 > PM09 > PM08 > PM07 > PM11 > PM13 > PM12 > PM05 > PM06 > PM10 > PM03 > PM04. The NIPI values indicates that the sediments are seriously or heavily polluted ($NIPI_{Nemerow} \geq 3.0$) in all sample and sampling point.

4.4.3 Geo-accumulation index (Igeo) and Enrichment factors (EF)

The Geo-accumulation Index (Igeo), was introduced by Müller (1969) to assess the level of metal accumulation in the sediments. It is mathematically expressed as follows:

$$\mathrm{Igeo} = \mathrm{Log}_2 \frac{Cn}{1.5 \times Bn}$$

Where, *Cn* refers to the measured concentration of metal ion in sample; *Bn* represents the background concentration value for element (Rudnick and Gao 2003) and 1.5 is the background matrix correction factor due to lithogenic effects. Müller (1969) classified Igeo into five groups as follows: Igeo < 0 = practically unpolluted, 0–1 = unpolluted to moderately polluted, 1–2 = moderately polluted, 2–3 = moderately to strongly polluted, 3–4 = strongly polluted, 4–5 = strongly to extremely polluted and Igeo > 5 = extremely polluted. According to Muller (1969) Scale, Igeo values (Igeo < 0) for majority of the elements (Au, Ag, Al, Ba, Bi, Cr, Cu, Ga, Rb, Mo,Ni, Sc, Sn, Sr, V, Y, Zn and Zr) in all sample (Table 8, Fig. 7), indicate minimal influence of anthropogenic pollution in the sediments which suggests that the sediments are in background value. Cd, Co, Fe, Pb, Th and U are unpolluted to moderately polluted (Igeo = 0–1), while Hg and U (samples PM07, PM10, PM11, PM13) are moderately polluted (Igeo = 1–2) in sediments. Th (samples PM07, PM09, PM11, PM13) is moderately to strongly polluted (Igeo = 2–4) and Hg (samples PM02, PM08, PM09) is extremely polluted (Igeo > 5) in the study area. Sediments were enriched with toxic metals such as Cd, Co Pb, Th, U and Hg.

The Enrichment factors (EF) of heavy metals has been commonly used to assess anthropogenic contamination. The EF values were calculated using the following equation (Abhijit and Ramkrishna 2017)

$$\mathrm{EF} = \frac{(\mathrm{me/Fe2O3})_{\mathrm{sample}}}{(\mathrm{me/Fe2O3})_{\mathrm{samplebackground}}}$$

Where $(me/Fe_2O_3)_{sample}$ is the measured ratio of metal between iron oxide and $(me/Fe_2O_3)_{sample\ background}$ unpolluted background ratio of metal of iron oxide. Five contamination categories were recognized on the basis of the enrichment factor (Lan et al. 2018) which are EF < 1, EF < 2, EF = 2–5, EF = 5–20 and EF = 20–40 corresponding to no enrichment, minimal enrichment, moderate enrichment, significant and severe enrichment (Yongming et al. 2016), respectively. The enrichment factors of heavy metals in the study area is showed in (Table 5, Fig. 8). U possesses the highest EF value (1221) in sample PM11, Hg (1047) is the second most abundant enriched element in sample PM11 and Y (740.67) is the third abundant enriched element in sample PM11 in the study area. Ag, Ba and Rb show no enrichment (EF < 1) in all samples. Al and Ni was in the category of minimal enriched (EF < 2). Cr, Ga, Mo, Sr, Th and Zr generally show moderate enrichment (EF = 2–5). Au (PM03,PM05, PM06 and PM11), Bi, Cd, Co,Cu, Fe, Pb, Sc, Sn, U, V and Zn are significantly enriched (EF = 5–20) and Au (PM02), Bi (PM09 to PM11), Hg, Zr (PM03) and U and Y (PM07 to PM13) are in the class of severe enrichment (EF = 20–40). Moderately to severely enrichment of some heavy metals in the study area indicates its origin from the anthropogenic sources such as mining, urbanization, household effluents, phosphate fertilizers, agrochemicals, industrial wastes deposition and agricultural practices in the study area.

Table 5
Computed enrichment factor (EF) of heavy metals in stream sediments of Pouma area

	PM02	PM03	PM04	PM05	PM06	PM07	PM08	PM09	PM010	PM011	PM012	PM013
Au	92.49	14.85	1.27	16.12	11.32	3.06	0.60	2.16	0.67	9.36	0.46	1.08
Ag	0.39	0.09	0.01	0.16	0.11	0.02	0.02	0.02	0.01	0.09	0.01	0.02
Al	1	1	1	1	1	1	1	1	1	1	1	1
Ba	0.19	0.48	0.37	0.38	0.32	0.26	0.38	0.25	0.30	1.31	0.49	0.48
Bi	6.07	10.24	7.20	13.21	10.97	10.31	11.00	41.25	14.04	57.75	22.92	13.21
Cd	12	11	8	27	32	12	34	22	29	17	16	34
Co	9.22	5.68	4.08	3.67	2.70	9.54	28.74	3.18	3.34	14.24	4.87	4.01
Cr	3.92	5.70	5.48	3.94	3.60	13.15	19.13	4.07	4.18	8.37	5.18	4.60
Cu	8.67	7.02	11.57	4.53	2.37	5.40	45.18	117.86	3.32	19.25	5.24	3.34
Fe	9.66	18.27	14.16	13.60	10.64	20.68	43.00	10.65	12.22	15.28	16.44	12.82
Ga	5.56	5.56	3.87	3.07	2.53	0.20	5.86	0.36	1.83	0.18	2.83	1.24
Hg	508	190	72	399	238	391	572	744	244	1047	557	338
Mo	2.14	1.79	1.70	4.94	3.72	9.00	13.40	7.40	7.29	16.80	5.33	4.67
Ni	1.18	1.32	1.32	0.77	0.66	2.05	8.24	0.84	0.89	3.28	1.01	1.03

Table 5
Continued

Pb	15.02	103.89	6.52	18.12	8.14	26.04	23.81	21.09	15.85	132.26	18.55	18.30
Rb	0.15	0.27	0.57	0.14	0.12	0.20	0.18	0.13	0.15	0.92	0.22	0.18
Sc	9.51	10.77	5.45	9.92	12.11	10.41	11.16	10.53	10.77	12.10	12.05	10.78
Sn	8.06	15.76	34.88	7.19	4.18	23.44	27.97	47.04	8.10	52.07	12.22	6.90
Sr	4.60	4.63	2.03	2.78	2.45	0.57	0.85	1.37	2.47	1.44	3.06	2.25
Th	4.60	4.63	2.03	2.78	2.45	0.57	0.85	1.37	2.47	1.44	3.06	2.25
U	8	18	8	44	65	321	34	213	175	1221	159	215
V	6.72	7.43	6.38	4.36	4.02	14.74	19.28	3.86	4.96	7.94	6.43	4.98
Y	10.70	15.01	7.06	16.10	16.99	28.02	15.61	24.93	22.76	740.67	26.71	25.88
Zn	4.58	11.88	5.11	8.34	5.62	6.69	8.31	4.93	6.90	8.73	9.85	6.94
Zr	12.51	29.03	2.98	5.19	2.69	0.28	3.83	0.21	0.85	0.64	2.26	0.67

4.4.4 Ecological risk factor (Er), Potential ecological risk index (RI) and anthropogenic metal input

This is an index that quantitatively expresses the potential ecological risk associated with a given single contaminant (Hakanson et al. 1980). It is calculated as follows:

$ErF = Tr^i \times CF^i$

Where Tr^i is toxic response factor of a metal (Pb = 5, Zn = 1, Cd = 30, Cr = 2, Ni = 5) and CF^i is the contamination factor (Hakanson et al. 1980). Five terminologies are used to define ecological risks based on Hakanson et al. (1980). These are < 40, low potential ecological risk; 40 < 80, moderate potential ecological risk; 80 < 160, considerable potential ecological risk; 160 < 320, high potential ecological risk; and ≥ 320, very high ecological risk. The Er varies from 0.111 (Cr and Ni) in sample PM09 and PM11 to 1464 (Hg) in sample PM02 (Table 6, Fig. 9). The Er in sediments showed low ecological risk factor (Er < 40) for Cd, Co, Cu, Cr, Ni, Pb and U (PM02 to PM04) with low potential ecological risk factor (Er < 40) in all the studied sites, which apparently showed less potential ecological impact on living biota. U is generally moderate to considerable potential ecological risk factor (Er = 40 > 320) in the study area. Hg (PM03, PM04, PM10 and PM11), U (PM10, PM13 and PM12) shows high potential ecological risk factor (Er = 160 < 320) and Hg and U (PM07, PM09 and PM11) have very high potential ecological risk factor (Er ≥ 320).

Table 6
Ecological risk factor (Er) and Potential ecological risk index (RI) of heavy metals in sediments of Pouma area

	PM02	PM03	PM04	PM05	PM06	PM07	PM08	PM09	PM010	PM011	PM012	PM013	RI
Cd	26.67	10.00	16.67	26.67	50.00	13.33	46.67	30.00	26.67	3.33	13.33	33.33	297
Co	4.65	1.21	1.98	0.85	0.97	2.43	9.14	1.01	0.73	0.65	0.93	0.93	25
Cr	0.57	0.35	0.76	0.26	0.37	0.96	1.74	0.37	0.26	0.11	0.28	0.30	6
Cu	3.13	1.07	4.02	0.75	0.61	0.98	10.27	26.79	0.52	0.63	0.71	0.55	50
Hg	1464	232	200	528	488	568	1040	1352	304	272	608	448	7504
Ni	0.26	0.12	0.27	0.08	0.10	0.22	1.12	0.11	0.08	0.06	0.08	0.10	3
Pb	5.41	15.85	2.26	3.00	2.09	4.74	5.41	4.79	2.47	4.29	2.53	3.03	56
U	23	23	23	61	140	490	65	408	229	333	182	299	2276
V	0.97	0.45	0.89	0.29	0.41	1.07	1.75	0.35	0.31	0.10	0.35	0.33	7
Zn	0.33	0.36	0.36	0.28	0.29	0.24	0.38	0.22	0.21	0.06	0.27	0.23	3

The Potential ecological risk index (RI) is the sum of all the ecological risk factors of the metals under study, taking into account the cumulative effects of the metals under study (Hakanson et al. 1980; Liu et al. 2020). It is calculated thus:

$$\mathrm{RI} = (\mathrm{ErF1} + \mathrm{ErF2} + \mathrm{ErF3} \cdots + \mathrm{ErFn})$$

Where ErF is the ecological risk factor and n is the number of elements studied. The following terminologies have been used for the potential ecological risk index: < 150, low ecological risk; 150 < 300, moderate ecological risk; 300 < 600, considerable ecological risk; and ≥ 600, very high ecological risk. The results of potential ecological risk index is presented in Table 10, Fig. 6. RI in the study area is in the order: Hg > U > Cd > Pb > Cu > Co > V > Cr > Ni > Zn with values 7504, 2276, 297, 56, 50, 25, 7, 6, 3 and 3 respectively. Hg has the highest RI value, second by U and third by Cd in sediments of the study area. Pb, Cu, Co, V, Cr, Ni and Zn had low ecological risk index while Cd has moderate ecological risk index in the study area. Hg and U shows very high ecological risk index across the study area.

The anthropogenic metal input in tailings is derived from the following formula:

Anthropogenic Input = $\frac{X - X_1}{X_1} \times 100$

Where, x represents the average concentration of the metal in sediments, and x_1 is the average background concentration of the metal (Rudnick and Gao 2003). The results of anthropogenic input are presented in Table 7 and Fig. 11 below. Anthropogenic input of metals varies from 0.03 (Ag) in samples PM10 and PM12 to 3660 (Hg) in sample PM02. Anthropogenic input refers to Cu (sample PM09), Pb

(samples PM02, PM03, PM08), Sn (samples PM04, PM08, PM09) Y (sample PM11), Hg, Th and U in the study area. This may be due to mining activities (quarrying), agricultural practices, used of phosphate fertilizers, pesticides, fungicides, sewage sludge, garbage, assorted waste, municipal waste and effluents from household discharge into various streams of the study area.

Conclusion

This work was aimed at assessing the distribution of trace and rare earth elements and level of pollution in stream sediments of Pouma area. The slight enrichment of Fe_2O_3 in sediments indicate that the sediments are highly ferruginous and should come from a ferromagnesian mineral. Strongly positive correlation coefficients indicate a common source. Er values are low for Cd, Co, Cu, Cr, Ni and Pb with low potential ecological risk factor in the study area, with high potential ecological risk factor for U and Hg. The study area shows low potential ecological risk index to extreme ecological risk index. The PLI, EF, NIPI and RI of Au, Ag, Al, Ba, Bi, Cd, Co, Cu, Cr, Fe, Hg, Ga, Mo, Nb Ni, Pb, Rb, Sc, Sn, Sr, Th, U, V, Y, Zn and Zr indicate metal pollution of sediments in the Pouma area. Natural and anthropogenic metal input assessment reveals that the dominantly mafic lithologies in the area, mining and domestic activities as well as agricultural activities of Pouma area are the main source of metal contamination.

Declarations

Acknowledgments This study is a part of the first author Msc thesis research work at the University of Buea. We gratefully acknowledge the editors for the handling of the manuscript.

Funding The authors declare that no funds, grants, or other support were received during the preparation of this manuscript.

Competing Interests The authors have no relevant financial or non-financial interests to disclose.

Author's contributions All authors contributed to the study conception and design. Material preparation, data collection and analysis were performed by Ndema Mbongue Jean-Lavenir, Tume Noela Kiki and Godlove Muh Ndi. The first draft of the manuscript was written by Tume Noela Kiki and Lemnyuy Prosper Yiika and all authors.

Data Availability Statements The Datasets generated during and/or analysed during the current study are available from the corresponding author on reasonable request.

References

1. Abhijit M, Ramkrishna M (2017) Geochemical contamination in the mine affected soil of Raniganj Coalfielde a river basin scale assessment. Geosci Frontiers, 30:1-14. DOI: 10.1016/j.gsf.2017.10.011
2. Adeel M., Lee JY, Zain M, Rizwan M, Nawab A, Ahmad MA, Shafiq M, Yi H, Jilani G, Javed R, Horton R, Rui Y, Tsang D, Xing B (2019) Cryptic footprints of rare earth elements on natural resources and living organisms. Environment international, 127:785–800. https://doi.org/10.1016/j. envint.2019.03.022
3. El-Taher A, Uosif MAM (2006) The Assessment of the Radiation Hazard Indices due to Uranium and Thorium in Some Egyptian Environmental Matrices. Journal of Physics. D: Applied Physics. 39.
4. Argyraki A, Kelepertzis E, Botsou F, Paraskevopoulou V, Katsikis I, Trigoni M. (2018) Environmental availability of trace elements (Pb, Cd, Zn, Cu) in soil from urban, suburban, rural and mining areas of Attica. Hellas Journal of Geochemical Exploration, 187(2018):201–213. https://doi.org/10.1016/j.gexplo.2017.09.004
5. Betsi TB, Ngo Bidjeck LMB, Mvondo H, Mama Nga LNY, Molotouala CA, McFarlane C (2020) Rutile LA-ICP-MS U-Pb geochronology and implications for tectono-metamorphic evolution in the Yaoundé Group of the Neoproterozoic Central African Orogeny. J Afr Earth Sci, 171:103–939. https://doi.org/10.12691/jgg-5-62
6. Caeiro S, Costa MH, Ramos T, Fernandes F, Silveira N, Coimbra A, Medeiros G, Painho M (2005) Assessing heavy metal contamination in Sado Estuary sediment: an index analysis approach. Ecol Ind 5(2):151–169
7. Chan WS, Routh J, Luo C, Dario M, Miao Y, Luo D, Wei L (2021) Metal accumulations in aquatic organisms and health risks in an acid mineaffected site in South China. Environmental geochemistry and health, 43(11):4415–4440. https:// doi.org/10.1007/s10653-021-00923-0
8. Chung SY, Venkatramanan S, Park KH, Son JH, Selvam S (2018) Source and remediation for heavy metals of soils at an iron mine of Ulsan City, Korea. Arab J Geosci 11:769

9. Castaing C, Feybesse Jl, Thieblemont D, Triboulet C, Chevremont P (1994) Palaeogeographical reconstructions of the Pan-African/Brasiliano orogen: closure of an oceanic domain or intracontinental convergence between major blocks. – Prec Res, 69: 327-344
10. Emmanuel A, Cobbina SJ, Adomako D, Duwiejuah AB, Asare W (2014) Assessment of heavy metals concentration in soils around oil filling and service stations in the Tamale Metropolis. Afri J Environ Sci Techn, 8:256-266. DOI: 10.5897/AJEST2014.1664
11. Etame J, Tchameni Ngouabe EG, Ngon Ngon GF, Ntamak-Nida MJ, Suh CE, Bilong MGP (2013) Mineralogy and geochemistry of active stream sediments from the Kelle River drainage system (Pouma, Cameroon). Sci Technol Dév 14:35–47 65.
12. Gao J, Du F, Li W, Han J, Wang X, Bao J et al. (2016) Content and accumulation characteristics of heavy metals in dominant plants in Xiao Bai He Area of the Yellow River Wetland. J Agro-Environ Sci, 35 (11):2180–2186. https://doi.org/10.11654/jaes.2016-0335
13. Hakanson L (1980) An ecological risk index for aquatic pollution control. Sedimentol Approach Water Res 14(8):975–1001
14. Hannigan RE, Sholkovitz ER (2001) The development of middle rare earth element enrichments in freshwaters: Weathering of phosphate minerals. Chem. Geol. 175:495–508
15. Fuentes I, Márquez-Ferrando R, Pleguezuelos JM, Sanpera C, Santos X (2020) Long-term trace element assessment after a mine spill: Pollution persistence and bioaccumulation in the trophic web. Environmental Pollution 267, 115406
16. Fuh CG, Nkoumbou C, Numbem JT, Mukete KO, Tchouankoue JP (2021a) Petrology, geochemistry, Ar–Ar isotopes of an arc related calk-alkaline pluton from Mamb (Pan-African Yaounde group, Cameroon): A testimony to the subduction of a hot oceanic crust. Lithos, 384-385, 105973. https://doi.org/10.1016/j. lithos.2021.105973
17. Khadijeh SRI, Elias SB,Wood KA, Reza AM (2009) Rare earth elements distribution in marine sediments of Malaysia coasts. J Rare Earths 27(6):1066–1077
18. Kaiser HF (1958) The varimax criterion for analytic rotation in factor analysis. Psychometrika, 23:187-200
19. Lan XL, Ning, ZP, Xiao QX, Huang ZY, Liu YZ, Xiao TF, Zhao, YL, Shi-Liang WU (2018): Spatial distribution, sources and bioavailability of heavy metals in the surface sediments of longjiang river, southern china. Environ. Sci. 39:748–757
20. Lecuyer C, Reynard B, Grandjean P (2004) Rare earth element evolution of Phanerozoic seawater recorded in biogenic apatites. Chem. Geol. 204:63–102
21. Li XH, Chen Y, Tchouankoue JP, Liu CZ, Li J, Ling XX, Tang GQ Liu Y (2017) Improving geochronological framework of the Pan-African orogeny in Cameroon: New SIMS zircon and monazite U-Pb age constraints. Prec Res, 294:307–321. https://doi.org/10.1016/j.precamres.2017.04.006
22. Liu H, Xie Y, Li J, Zeng G, Li H, Xu F, Feng S, Xu H (2020) Effect of Serratia sp. K3 combined with organic materials on cadmium migration in soil-vetiveria zizanioides L. system and bacterial community in contaminated soil. Chemosphere 242:125-164
23. Liu H, Guo H, Pourret O, Wang Z, Sun Z, Zhang W, Liu M (2021) Distribution of rare earth elements in sediments of the North China Plain: A probe of sedimentation process. Appl. Geochem. 134:105089.
24. Loell M, Albrecht C, Felix-Henningsen P (2011) Rare earth elements and relation between their potential bioavailability and soil properties, Nidda catchment (Central Germany). Plant Soil. 349: 303–317
25. McLennan SM, Taylor SR (2001) Hemming, composition, differentiation and evolution of continental crust: Constraints from sedimentary rocks and heat flow, in Evolution and Differentiation of the Continental Crust, edited by Brown M, Rusher T Cambridge Univ. Press, New York, in press
26. Moiseenko TI, Dinu MI, Gashkina NA, Kremleva TA (2019): Aquatic environment and anthropogenic factor effects on distribution of trace elements in surface waters of European Russia and Western Siberia. Environmental Research Letters 14, 065010
27. Müller G (1981) The heavy metal content of the sediments of the Neckar and its tributaries: An inventory. Chemische Zeitung, 105:157-164
28. Nkoumbou C, Barbey P, Yonta-Ngoune C, Paquette JL, Villieras F (2014) Precollisional geodynamic context of the southern margin of the Pan-African fold belt in Cameroon. J Afr Earth Sci 99:245–260. https://doi.org/10.1016/j. jafrearsci.2013.10.002
29. Ndjigui PD, Fadil-Djenabou S, Beauvais A, Ambrosi JP (2014) Origin and evolution of Ngaye River alluvial sediments, Northern Cameroon: geochemical constraints. J Afri Earth Sci 100:164–178
30. Nesbitt HW, Young GM, McLennan KRR (1996) Effects of chemical weathering and sorting on the petrogenesis of siliciclastic sediments, with implications for provenance studies. J Geol 104:525–542
31. Nédelec A, Macaudière J, Nzenti JP. Barbey P (1986) Evolution métamorphique et structurale des schistes de Mbalmayo (Cameroun). Implications pour la structure de la zone mobile panafricaine d'Afrique centrale, au contact du craton du Congo. Comptes Rendus de l'Académie des Sciences de Paris 303:75–80.

32. Nzenti JP, Barbey P, Macaudiere J, Soba D (1988) Origin and evolution of the late Precambrian high-grade Yaoundé gneisses (Cameroon). Prec Res 38:91–109. https://doi.org/10.1016/0301-9268(88)90086-1
33. Otari M, Dabiri R (2015) Geochemical and environmental assessment of heavy metals in soils and sediments of Forumad Chromite mine, NE of Iran. J Min Environ 6:251-261
34. Owona S, Schulz B, Ratschbacher L, Mvondo OJ, Ekodeck GE, Tchoua FM, Affaton P (2011) Pan-African metamorphic evolution in the southern Yaoundé Group (Oubanguide Complex, Cameroon) as revealed by EMPmonazite dating and thermobarometry of garnet metapelites. J Afri Earth Sci 59:125–139. https://doi. org/10.1016/j.jafrearsci.2010.09.003
35. Owens PN, Walling DE, He Q, Shanahan J, Foster IDL (1997) The use of caesium-137 measurements to establish a sediment budget for the Start catchment, Devon, UK. Hydrol Sci J 42:405–423. DOI:https://doi.org/10.1080/ 02626669709492037
36. Pejman A, Bidhendi GH, Ardestani M, Saeedi M, Baghvand A (2015) A new index for assessing heavy metals contamination in sediments: A case study. Ecological Indicators 58:365–373
37. Poidevin JL (1991) Les ceintures de roches vertes de la République Centrafricaine. Contribution à la connaissance du précambrien du nord du craton du Congo. Thèse de Doctorat d'Etat, Université Blaise Pascal, Clermont-Ferrand, France.
38. Ramos-Vázquez MA, Armstrong-Altrin JS, Machain-Castillo ML, GíoArgáez FR (2018) Foraminiferal assemblages, 14C ages, and compositional variations in two sediment cores in the western Gulf of Mexico. J S Am Earth Sci 88:480–496
39. Rudnick RL, Gao S (2003) The composition of the continental crust. In: Holland, H.D. and Turekian, Crust, Elsevier- Program, Oxford, 1-64.http://dx.doi.org/10.1016/b0-08-043751-6/03016-4
40. Singh H, Singh D, Singh SK, Shukla DN (2017) Assessment of river water quality and ecological diversity through multivariate statistical techniques, and earth observation dataset of rivers Ghaghara and Gandak, India. Int J River Basin Manag, pp 1–14. doi:10.1080/15715124.2017.1300159
41. Sholkovitz ER (1995) The aquatic chemistry of rare earth elements in rivers and estuaries. Aquat Geochem. 1:1–34
42. Sojka M, Choinski A, Ptak M, Siepak M (2020) The variability of lake water chemistry in the Bory Tucholskie National Park (Northern Poland). Water 12, 394
43. Taati A, Salehi MH, Mohammadi J, Mohajer R, Díez S (2020) Pollution assessment and spatial distribution of trace elements in soils of Arak industrial area, Iran: Implications for human health. Environ Res 187, 109577
44. Tomlinson DL, Wilson JG, Harris CR, Jeffrey DW (1980) Problems in the assessment of heavy-metal levels in estuaries and the formation of a pollution index. Helgol Meeresunters 33(1):566. https:// doi.org/10.1007/bf024 14780
45. Torres-Alvarado IS, Pandarinath K, Verma SP, Dulski P (2007) Mineralogical and geochemical effects due to hydrothermal alteration in the Los Azufres geothermal field, Mexico. Revista Mexicana de Ciencias Geológicas 24(1):15–24
46. Toteu SF, Van Schmus WR, Penaye J, Michard A (2001) New U-Pb and Sm-Nd data from north-central Cameroon and its bearing on the pre-Pan-African history of central Africa. Prec Res 108 (1-2):45–73. https://doi.org/10.1016/S0301- 9268(00)00149-2
47. Toteu SF, Penaye J, Poudjom Djomani Y (2004) Geodynamic Evolution of the Pan-African Belt in Central Africa with Special Reference to Cameroon. Can J Earth Sci, 41:73-85. https://doi.org/10.1139/e03-079
48. Toteu SF, Yongué Fouateu R, Penaye J, Tchakounté J, Semé Mouangué AC, Van Schmus WR, Deloule E, Stendal H (2006) U-Pb dating of plutonic rocks involved in the nappe tectonic in southern Cameroon: consequence for the Pan-African fold belt. J Afr Earth Sci, 44:479–493
49. Van Schmus WR, Oliveira EP, Da Silva Filho A.F, Toteu SF, Penaye J, Guimaraes IP (2008) Proterozoic links between the Borborema Province, NE Brazil, and the Central African Fold Belt: Geol Soc, London, Special Publications 294 (1):69–99. doi:10.1144/SP294.5
50. Wang W, Cawood PA, Pandit MK, Zhao JH, Zheng JP (2019) No collision between Eastern and Western Gondwana at their northern extent. Geology, 47(4):308–312. https://doi.org/10.1130/G45745.1
51. Wang X, Zhou D (2021) Spatial agglomeration and driving factors of environmental pollution: A spatial analysis. Journal of Cleaner Production 279, 123839
52. Yongming H, Peixuan D, Junji C, Posmentier ES (2006): Multivariate analysis of heavy metal contamination in urban dusts of Xi'an, Central China. Sci. Total Environ. 355: 176-186. DOI: 10.1016/j.scitotenv.2005.02.026
53. Zhang X, Zhang F, Chen X, Zhang W, Deng H (2012) REEs fractionation and sedimentary implication in surface sediments from eastern South China. Sea J Rare Earths, 30:614–620 Hu ZY, Haneklaus S, Sparovek G, Schnug E (2006) Rare earth elements in soils. Commun, Soil Sci Plant Anal 37:1381–1420

Figures

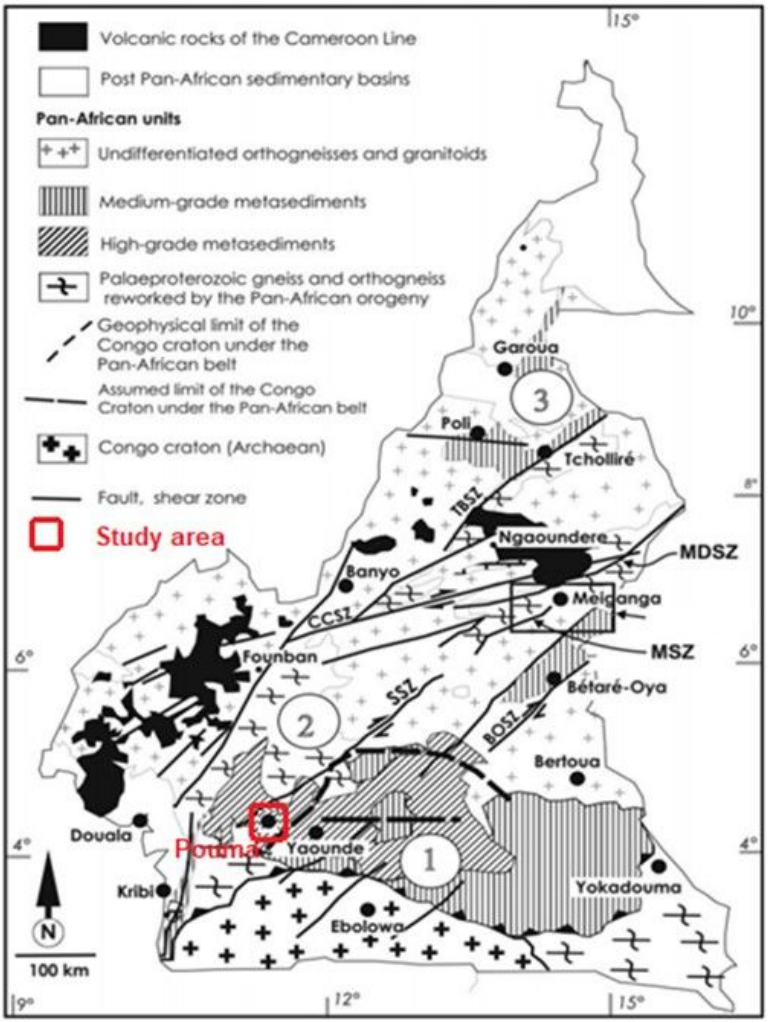

Figure 1

Geological map of Cameroon (modified from Toteu et al. 2001), showing major lithotectonic units and shear zones: (1) southern domain; (2) central domain; (3) northern domain; CCSZ, Central Cameroon shear zone; TBSZ, Tcholliré-Banyo shear zone; SSZ, Sanaga shear zone; BOSZ, Betaré Oya shear zone

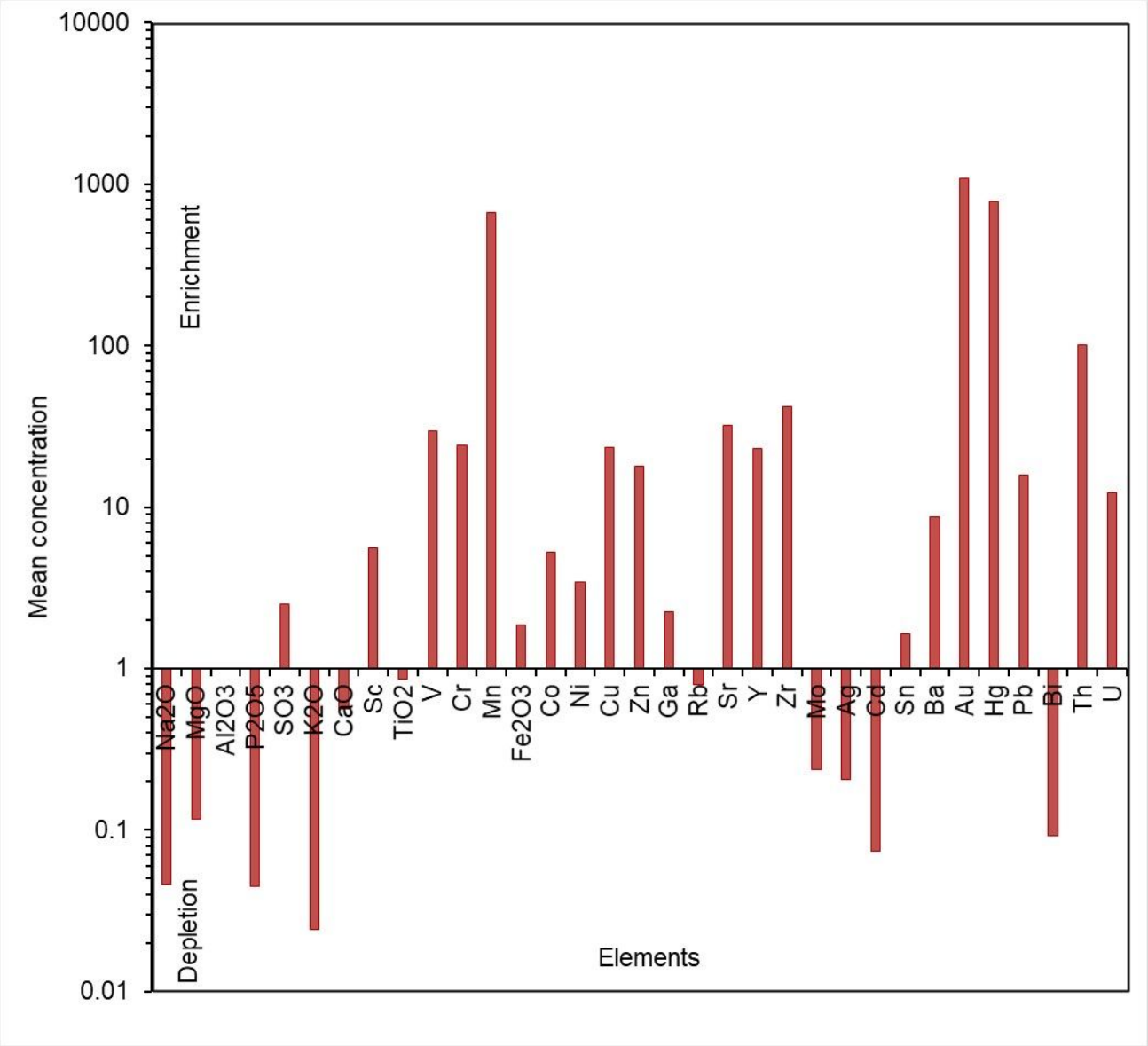

Figure 2

Enrichment-depletion plot for trace elements in sediments of Pouma area

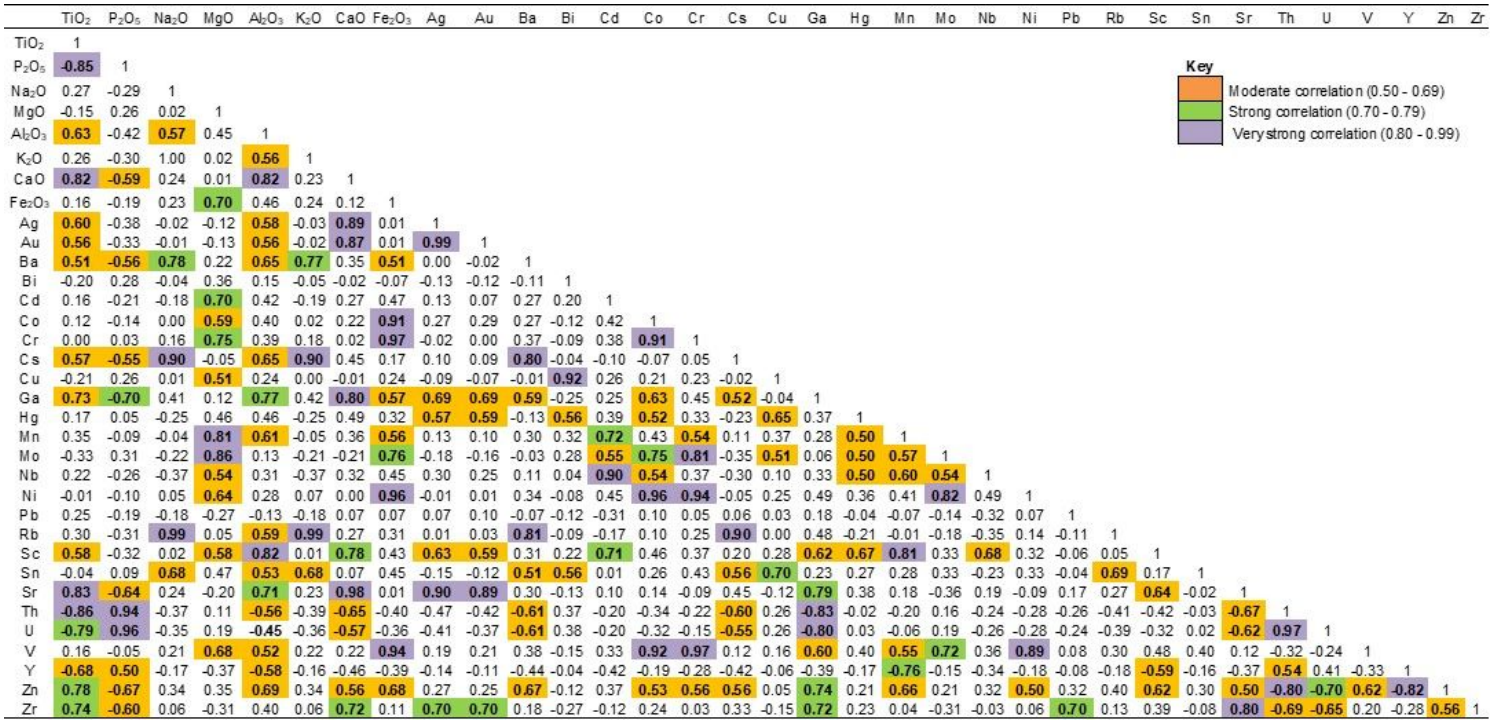

	TiO_2	P_2O_5	Na_2O	MgO	Al_2O_3	K_2O	CaO	Fe_2O_3	Ag	Au	Ba	Bi	Cd	Co	Cr	Cs	Cu	Ga	Hg	Mn	Mo	Nb	Ni	Pb	Rb	Sc	Sn	Sr	Th	U	V	Y	Zn	Zr
TiO_2	1																																	
P_2O_5	-0.85	1																																
Na_2O	0.27	-0.29	1																															
MgO	-0.15	0.26	0.02	1																														
Al_2O_3	0.63	-0.42	0.57	0.45	1																													
K_2O	0.26	-0.30	1.00	0.02	0.56	1																												
CaO	0.82	-0.59	0.24	0.01	0.82	0.23	1																											
Fe_2O_3	0.16	-0.19	0.23	0.70	0.46	0.24	0.12	1																										
Ag	0.60	-0.38	-0.02	-0.12	0.58	-0.03	0.89	0.01	1																									
Au	0.56	-0.33	-0.01	-0.13	0.56	-0.02	0.87	0.01	0.99	1																								
Ba	0.51	-0.56	0.78	0.22	0.65	0.77	0.35	0.51	0.00	-0.02	1																							
Bi	-0.20	0.28	-0.04	0.36	0.15	-0.05	-0.02	-0.07	-0.13	-0.12	-0.11	1																						
Cd	0.16	-0.21	-0.18	0.70	0.42	-0.19	0.27	0.47	0.13	0.07	0.27	0.20	1																					
Co	0.12	-0.14	0.00	0.59	0.40	0.02	0.22	0.91	0.27	0.29	0.27	-0.12	0.42	1																				
Cr	0.00	0.03	0.16	0.75	0.39	0.18	0.02	0.97	-0.02	0.00	0.37	-0.09	0.38	0.91	1																			
Cs	0.57	-0.55	0.90	-0.05	0.65	0.90	0.45	0.17	0.10	0.09	0.80	-0.04	-0.10	-0.07	0.05	1																		
Cu	-0.21	0.26	0.01	0.51	0.24	0.00	-0.01	0.24	-0.09	-0.07	-0.01	0.92	0.26	0.21	0.23	-0.02	1																	
Ga	0.73	-0.70	0.41	0.12	0.77	0.42	0.80	0.57	0.69	0.69	0.59	-0.25	0.25	0.63	0.45	0.52	-0.04	1																
Hg	0.17	0.05	-0.25	0.46	0.46	-0.25	0.49	0.32	0.57	0.59	-0.13	0.56	0.39	0.52	0.33	-0.23	0.65	0.37	1															
Mn	0.35	-0.09	-0.04	0.81	0.61	-0.05	0.36	0.56	0.13	0.10	0.30	0.32	0.72	0.43	0.54	0.11	0.37	0.28	0.50	1														
Mo	-0.33	0.31	-0.22	0.86	0.13	-0.21	-0.21	0.76	-0.18	-0.16	-0.03	0.28	0.55	0.75	0.81	-0.35	0.51	0.06	0.50	0.57	1													
Nb	0.22	-0.26	-0.37	0.54	0.31	-0.37	0.32	0.45	0.30	0.25	0.11	0.04	0.90	0.54	0.37	-0.30	0.10	0.33	0.50	0.60	0.54	1												
Ni	-0.01	-0.10	0.05	0.64	0.28	0.07	0.00	0.96	-0.01	0.01	0.34	-0.08	0.45	0.96	0.94	-0.05	0.25	0.49	0.36	0.41	0.82	0.49	1											
Pb	0.25	-0.19	-0.18	-0.27	-0.13	-0.18	0.07	0.07	0.07	0.10	-0.07	-0.12	-0.31	0.10	0.05	0.06	0.03	0.18	-0.04	-0.07	-0.14	-0.32	0.07	1										
Rb	0.30	-0.31	0.99	0.05	0.59	0.99	0.27	0.31	0.01	0.03	0.81	-0.09	-0.17	0.10	0.25	0.90	0.00	0.48	-0.21	-0.01	-0.18	-0.35	0.14	-0.11	1									
Sc	0.58	-0.32	0.02	0.58	0.82	0.01	0.78	0.43	0.63	0.59	0.31	0.22	0.71	0.46	0.37	0.20	0.28	0.62	0.67	0.81	0.33	0.68	0.32	-0.06	0.05	1								
Sn	-0.04	0.09	0.68	0.47	0.53	0.68	0.07	0.45	-0.15	-0.12	0.51	0.56	0.01	0.26	0.43	0.56	0.70	0.23	0.27	0.28	0.33	-0.23	0.33	-0.04	0.69	0.17	1							
Sr	0.83	-0.64	0.24	-0.20	0.71	0.23	0.98	0.01	0.90	0.89	0.30	-0.13	0.10	0.14	-0.09	0.45	-0.12	0.79	0.38	0.18	-0.36	0.19	-0.09	0.17	0.27	0.64	-0.02	1						
Th	-0.86	0.94	-0.37	0.11	-0.56	-0.39	-0.65	-0.40	-0.47	-0.42	-0.61	0.37	-0.20	-0.34	-0.22	-0.60	0.26	-0.83	-0.02	-0.20	0.16	-0.24	-0.28	-0.26	-0.41	-0.42	-0.03	-0.67	1					
U	-0.79	0.96	-0.35	0.19	-0.45	-0.36	-0.57	-0.36	-0.41	-0.37	-0.61	0.38	-0.20	-0.32	-0.15	-0.55	0.26	-0.80	0.03	-0.06	0.19	-0.26	-0.28	-0.24	-0.39	-0.32	0.02	-0.62	0.97	1				
V	0.16	-0.05	0.21	0.68	0.52	0.22	0.22	0.94	0.19	0.21	0.38	-0.15	0.33	0.92	0.97	0.12	0.16	0.60	0.40	0.55	0.72	0.36	0.89	0.08	0.30	0.48	0.40	0.12	-0.32	-0.24	1			
Y	-0.68	0.50	-0.17	-0.37	-0.58	-0.16	-0.46	-0.39	-0.14	-0.11	-0.44	-0.04	-0.42	-0.19	-0.28	-0.42	-0.06	-0.39	-0.17	-0.76	-0.15	-0.34	-0.18	-0.08	-0.18	-0.59	-0.16	-0.37	0.54	0.41	-0.33	1		
Zn	0.78	-0.67	0.34	0.35	0.69	0.34	0.56	0.68	0.27	0.25	0.67	-0.12	0.37	0.53	0.56	0.56	0.05	0.74	0.21	0.66	0.21	0.32	0.50	0.32	0.40	0.62	0.30	0.50	-0.80	-0.70	0.62	-0.82	1	
Zr	0.74	-0.60	0.06	-0.31	0.40	0.06	0.72	0.11	0.70	0.70	0.18	-0.27	-0.12	0.24	0.03	0.33	-0.15	0.72	0.23	0.04	-0.31	-0.03	0.06	0.70	0.13	0.39	-0.08	0.80	-0.69	-0.65	0.20	-0.28	0.56	1

Figure 3

Correlation matrix of major oxides in stream sediments of Pouma area

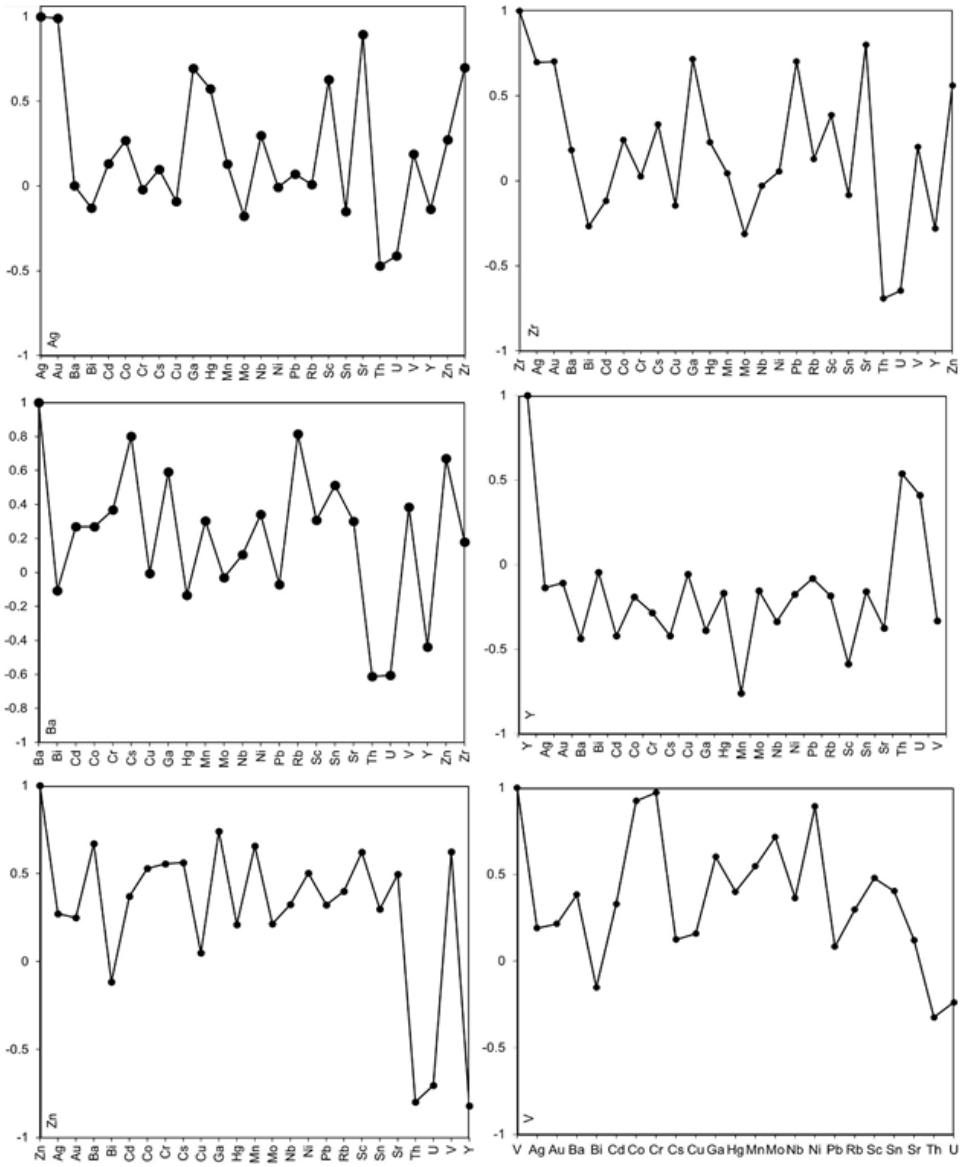

Figure 4

Selected correlation coefficient patterns of trace elements

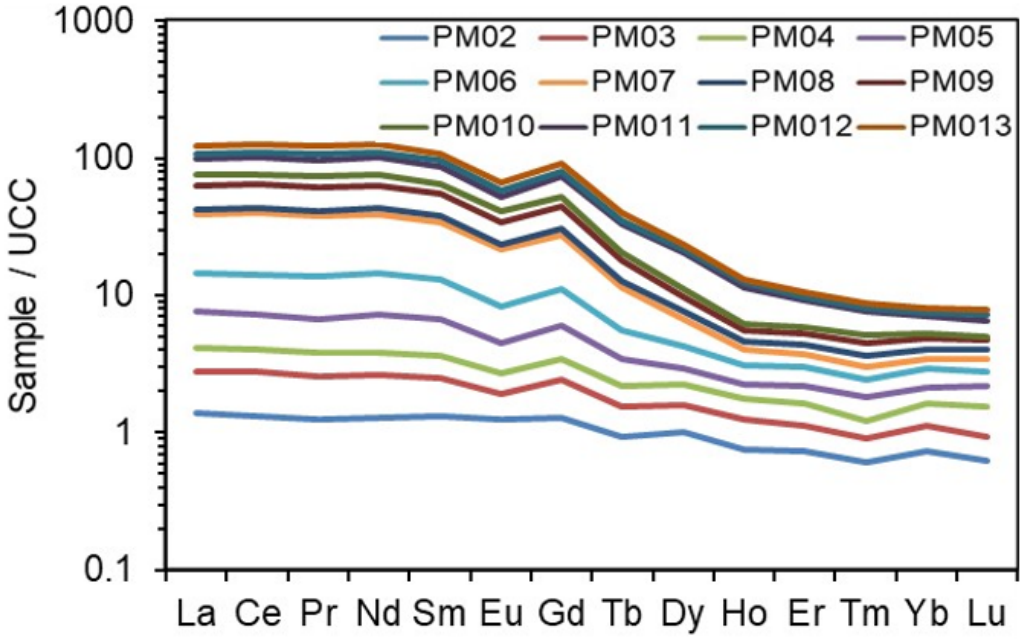

Figure 5

UCC-normalized rare earth elements. Normalization values are according to McLennan (2001)

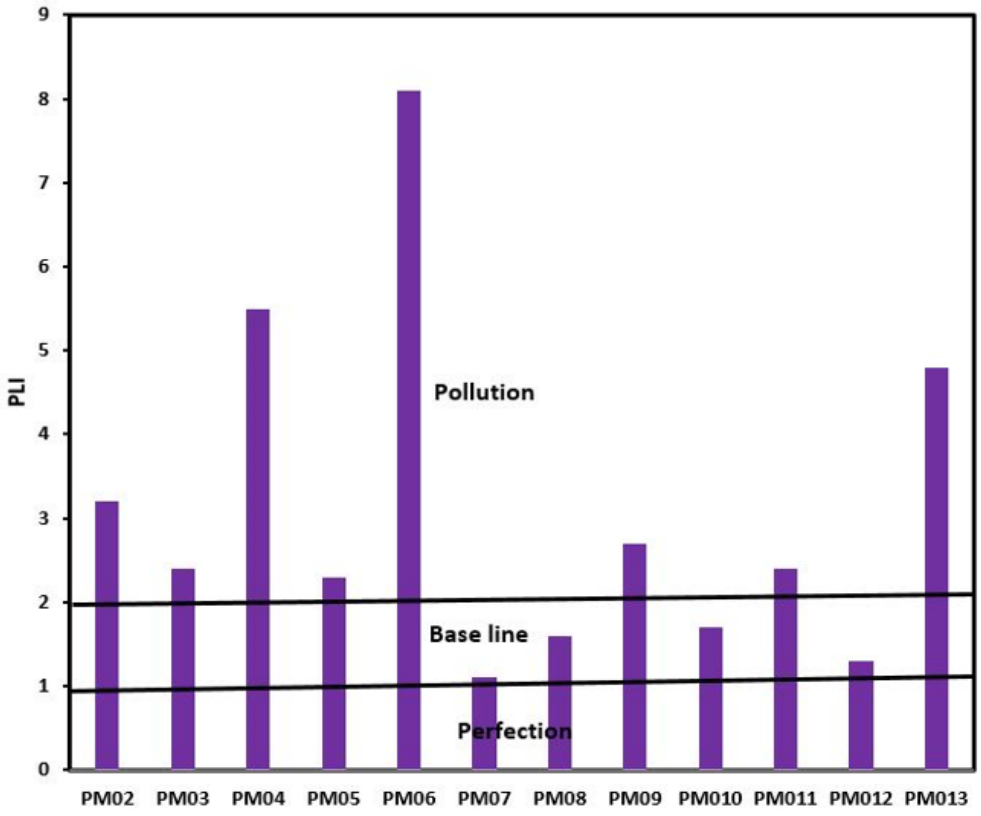

Figure 6

Pollution load index of heavy metals in stream sediments of Pouma area

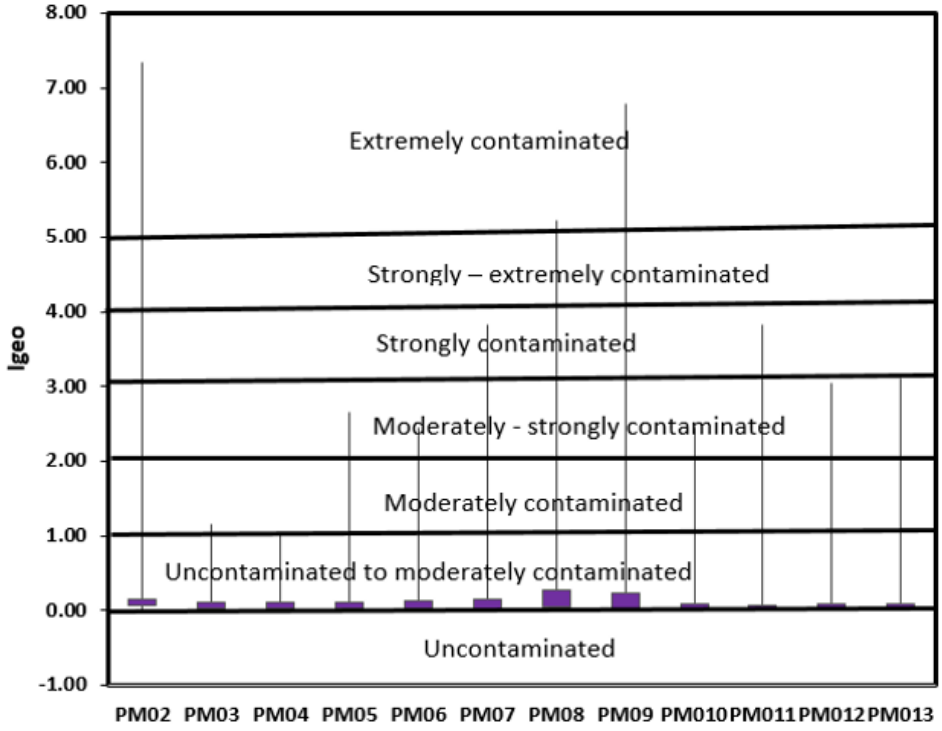

Figure 7

Geo-accumulation index plot of heavy metals in sediment of Pouma area

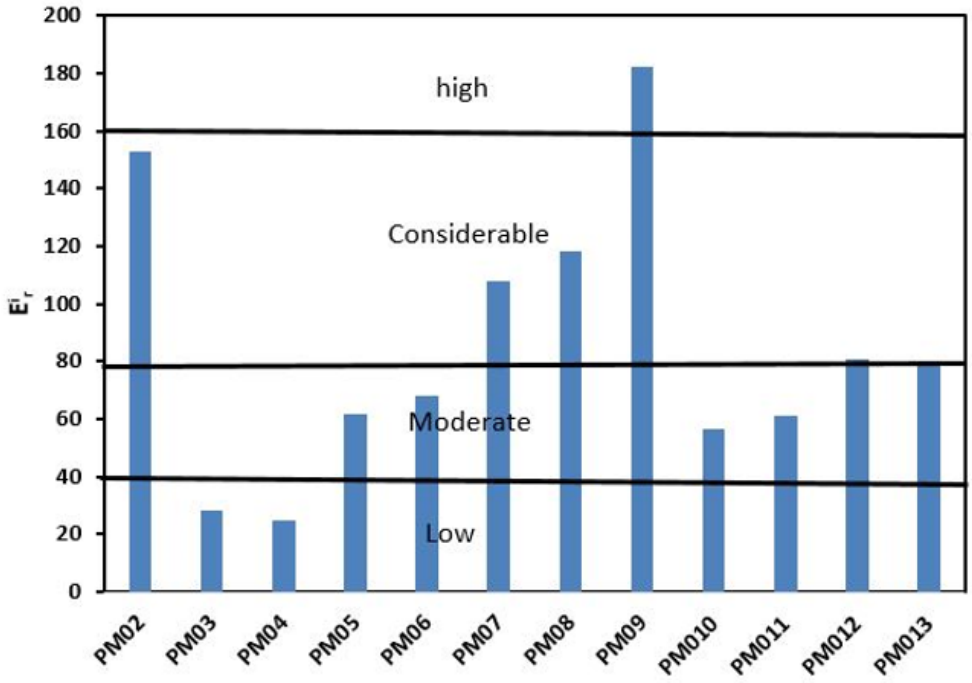

Figure 8

Plot of Enrichment factor of heavy metals in sediments of Pouma area

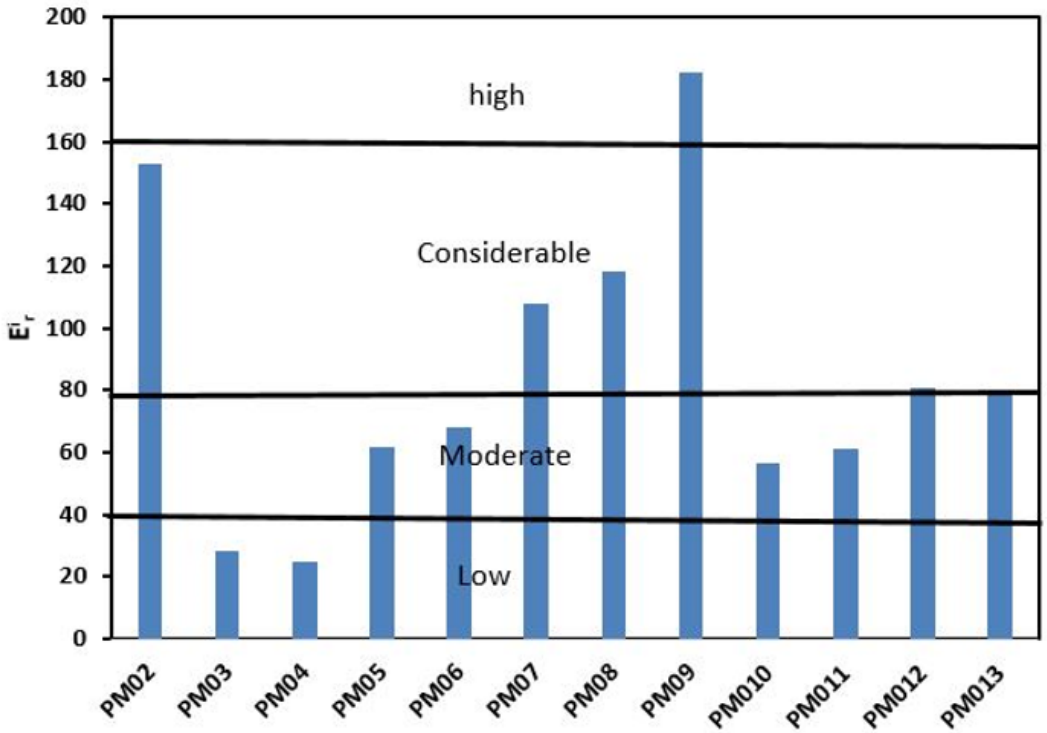

Figure 9

Graphical representation of ecological risk factor of heavy metals in stream sediments of Pouma area

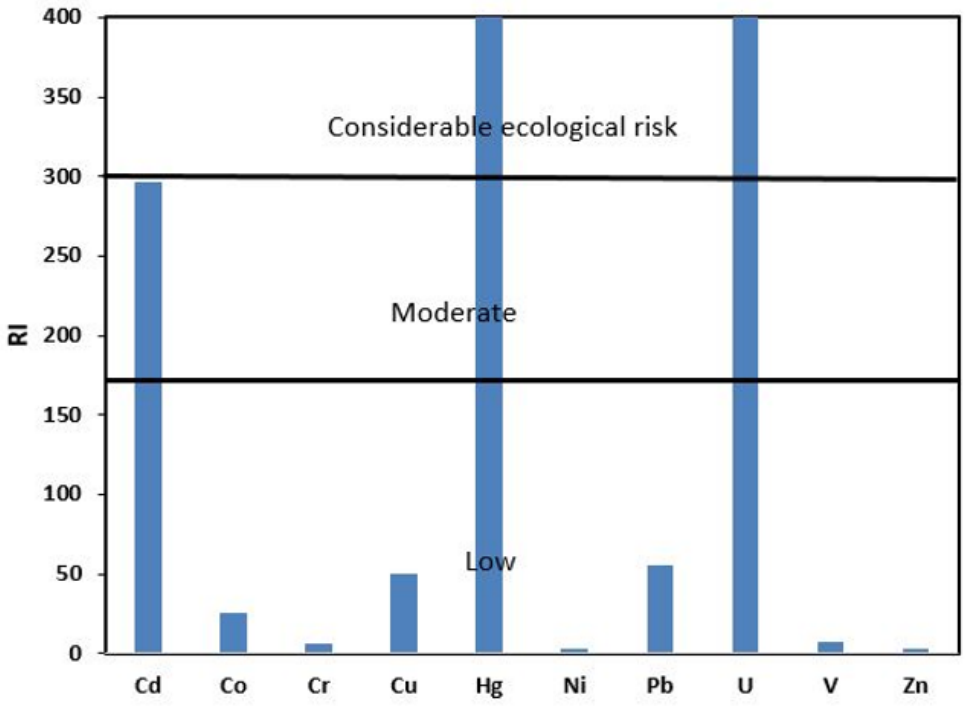

Figure 10

Plot of potential ecological risk index of heavy metals in stream sediments of Pouma area

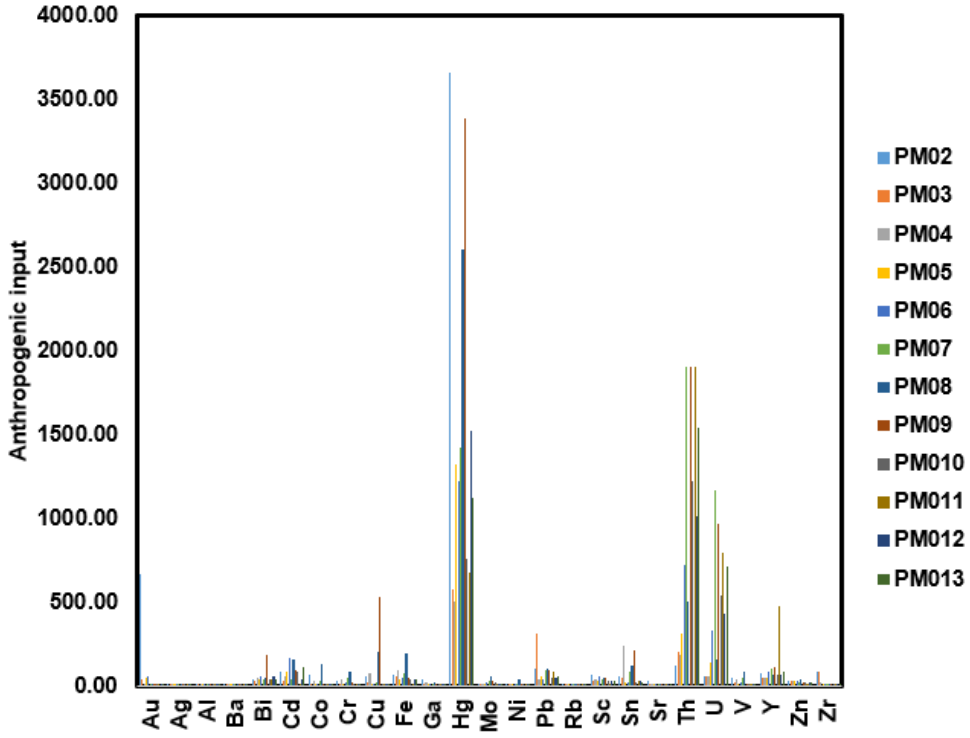

Figure 11

Histogram of anthropogenic input of heavy metals in sediments of Pouma area